



1 Motivation [1, 2]

Recently, we proposed a surface model for the charge of a dust particle in a plasma which avoids the unrealistic treatment of the grain surface as a perfect absorber for electrons and ions [1]. The charging of the dust particle is instead described as a physisorption process in the potential of the distorted region of the grain (see Fig. 1). For ions this potential is attractive on all length scales, because the grain is negatively charged, but for electrons it becomes attractive only at extremely small distances, where the polarization-induced part of the potential dominates the Coulomb repulsion.

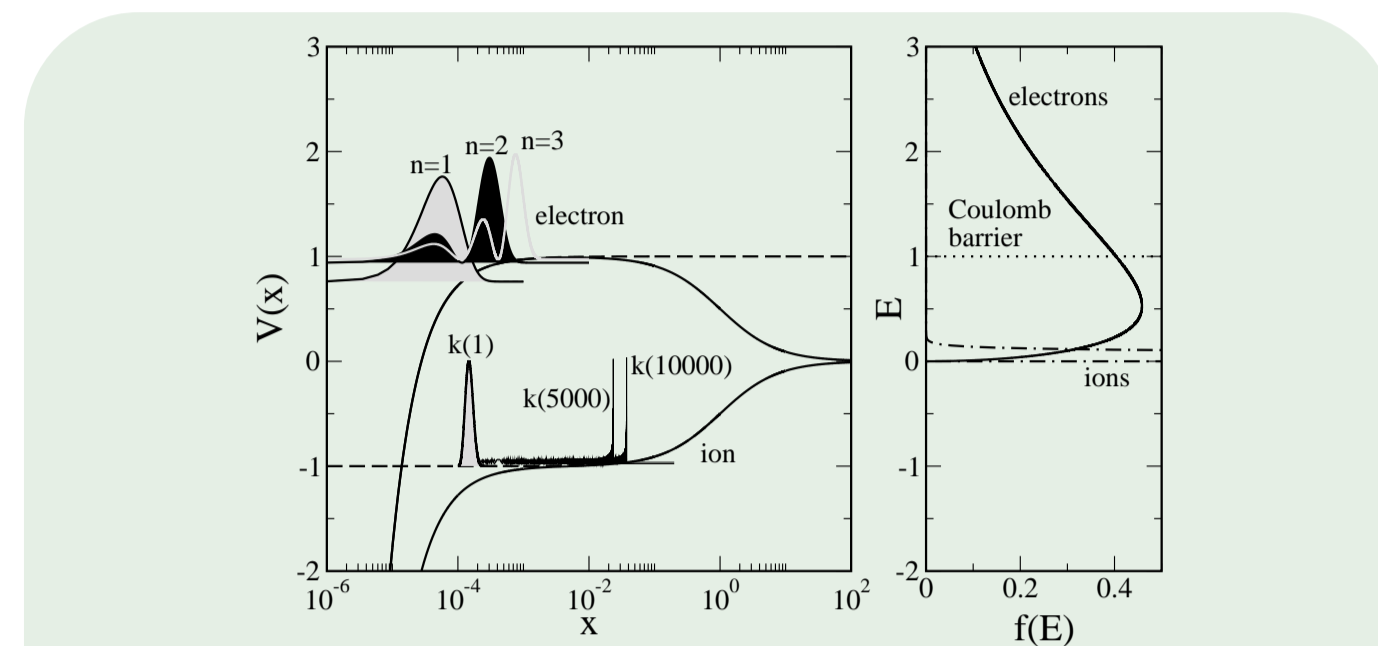


Fig. 1: Left panel: Potential energy for an electron (ion) in the field of a MF particle ($R = 4.7 \mu\text{m}$, $Z = 6800$) and representative probability distributions, $|u(x)|^2$, shifted to the binding energy and maxima normalized to one. Right panel: Bulk energy distribution functions for the helium discharge hosting the particle.

Provided ions get stuck in the attractive Coulomb tail of the grain potential, in trapped orbits, a few μm away from the grain surface, the grain charge is just the number of electrons quasi-bound in the polarization-induced surface states of the electron-grain interaction. Encapsulating the microphysics responsible for sticking into and desorption from these states into a sticking coefficient s_e and a desorption time τ_e an estimate for this number can be obtained by balancing on the grain surface the electron collection flux with the electron desorption flux (see Fig. 2). As a result [1],

$$Z_p = 4\pi R^2 s_e \tau_e j_e^{\text{OML}}(Z_p), \quad (1)$$

where the electron plasma flux is given by the orbital-motion limited electron flux and R is the grain radius.

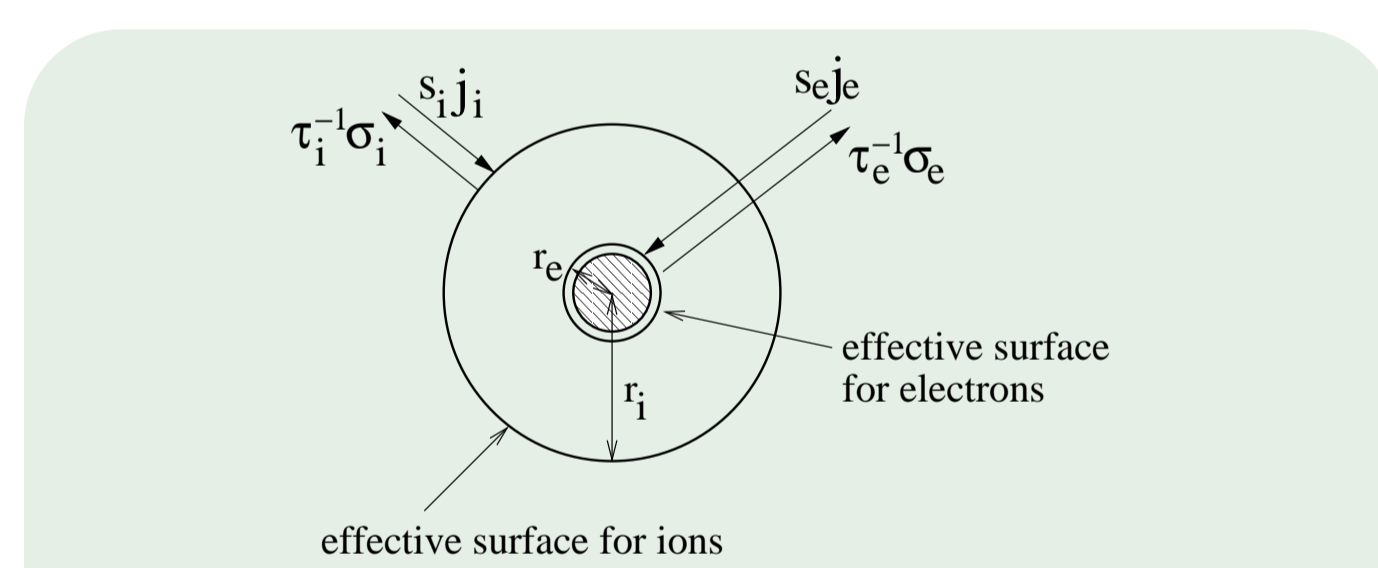


Fig. 2: Surface model for the distorted region of a grain with radius R . The quasi-stationary surface charges, $\sigma_{e,i}$, bound at $r_e \approx R$ and $r_i \approx r_e$, respectively, balance the plasma collection fluxes $s_{e,i} j_{e,i}^{\text{plasma}}$ with the respective desorption fluxes $\tau_{e,i}^{-1} \sigma_{e,i}$.

In [1] we approximated the product $s_e \tau_e$ by an Arrhenius-like expression,

$$s_e \tau_e = \frac{h}{k_B T_s} \exp\left[\frac{E_e^d}{k_B T_s}\right], \quad (2)$$

where E_e^d is the electron desorption energy and T_s is the grain temperature. Identifying $-E_e^d$ with the binding energy of the lowest polarization-induced (image) state and using T_s , due to lack of experimental data, as an adjustable parameter, we obtained excellent agreement with experimentally measured grain charges (see Fig. 3) [1, 2]. For a μm -sized grain in a low-temperature gas discharge $s_e \tau_e \approx 10^{-6}$ s.

The assumptions on which our model is based – ions not reaching the grain surface on the microscopic scale, instead quasi-bound a few μm in front of the grain surface, and electrons quasi-bound in external polarization-induced surface states – can be only justified by a complete microscopic calculation. The most pressing issues in this respect are a self-consistent calculation of the ion density surrounding a negatively charged grain and an explicit calculation of $s_e \tau_e$ from a microscopic model for the electron-grain interaction. In the following we present first results for the latter. A full description of our approach can be found in [3].

2 Theory [3]

As explained in [3], for the calculation of s_e and τ_e it suffices to consider, in a first approximation, a planar, uncharged plasma boundary. It defines the xy -plane of a coordinate system separating the plasma in the halfspace $z > 0$ from the solid in the halfspace $z \leq 0$.

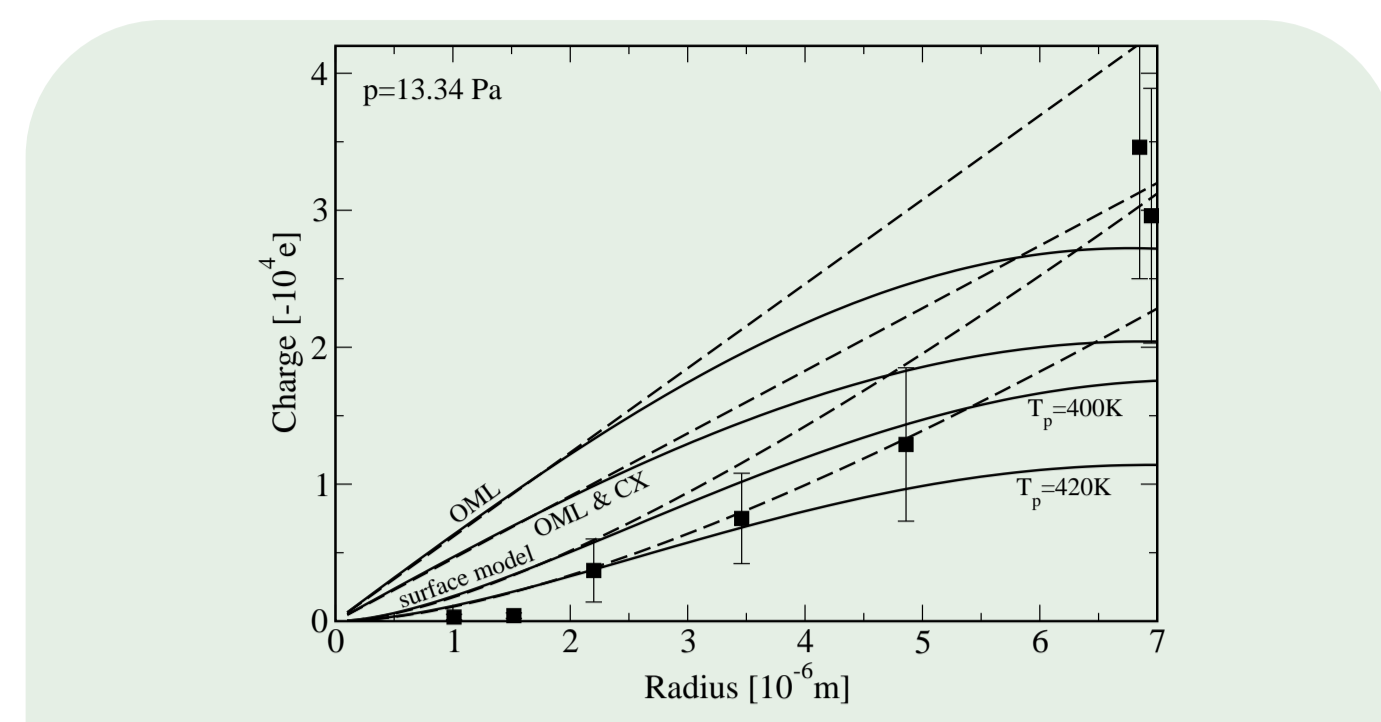


Fig. 3: Radius dependence of the charge of a MF particle in the sheath of an argon discharge. Squares are experimental data [E. B. Tomme et al., *Plasma Sources Sci. Technol.* **9**, 87 (2000)] and solid and dashed lines give, respectively, the charges obtained when the depletion of n_e in the confining sheath is included or not. For comparison, we also show the charges deduced from $j_e^{\text{OML}} = j_e^{\text{OML}}$ (OML) and from $j_e^{\text{OML}} = j_e^{\text{OML}} + j_e^{\text{CX}}$ (OML & CX) with $\sigma_{\text{CX}} = 0.72 \times 10^{-14} \text{cm}^2$.

The microphysics of electrons at an idealized metallic boundary, where the only surface modification due to the plasma is the build-up of surface charges, is schematically shown in Fig. 4. A plasma electron approaching the boundary in an extended state with $E > 0$ may be bound in a surface state with $E < 0$ provided it dissipates its excess energy to the internal electron-hole pairs of the metallic boundary. Similarly, an electron initially occupying a bound surface state may desorb from the surface when it gains enough energy to reach an extended state.

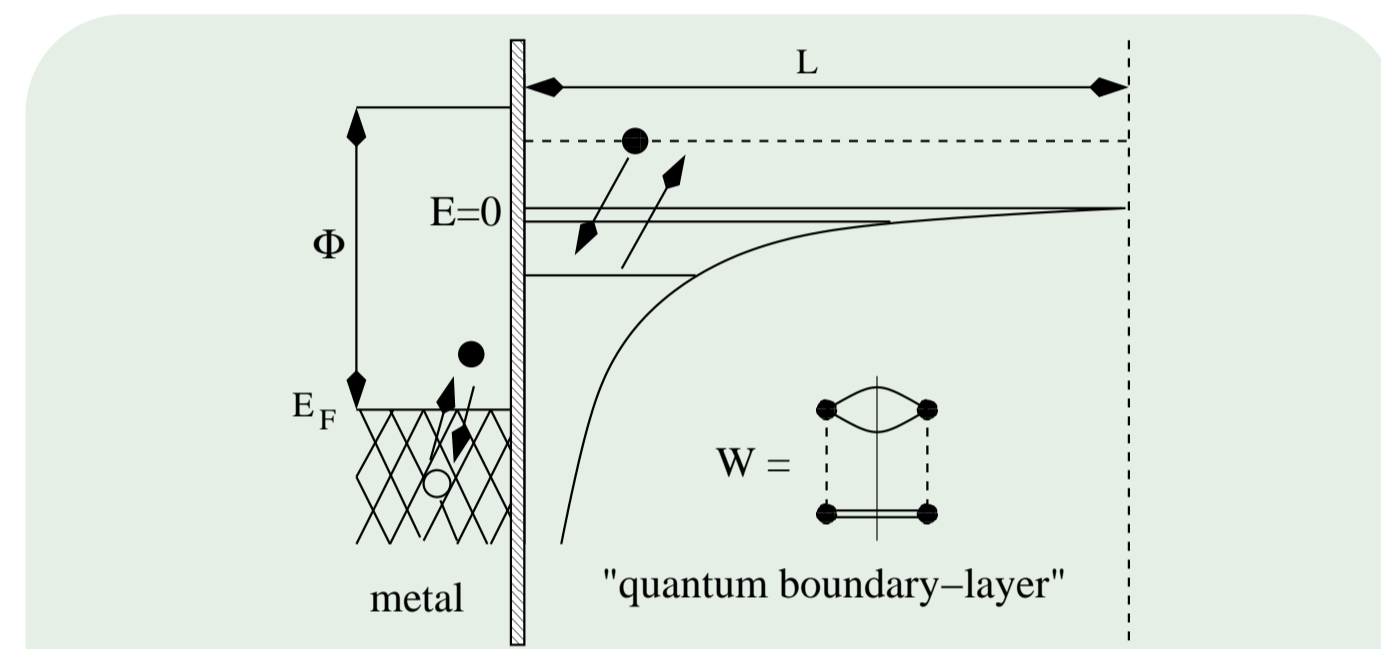


Fig. 4: Microphysics of plasma electrons at metallic boundaries. L is the width of the “boundary layer” where quantum mechanics applies; Φ and E_F , respectively, the work function and the Fermi energy of the metal.

Quite generally, a quantum-mechanical calculation of s_e and τ_e has to be based on a Hamiltonian,

$$H = H_e + H_b + H_{e-b}, \quad (3)$$

where H_e and H_b describe, respectively, the unperturbed dynamics of the plasma electrons in the vicinity of the solid and of the elementary excitations of the solid responsible for electron energy relaxation and H_{e-b} encodes the coupling between the two.

The electronic structure of a plasma boundary is rather complex. For instance, it cannot be expected that the boundary coincides with a crystallographic plane. More likely, the boundary is polycrystalline and consists of an irregular array of terraces. It may be also chemically modified due to the plasma. As a first step, we nevertheless assume a perfect boundary, applicable when the size of terraces is large and the chemical contamination is negligibly small.

Even then two types of surface states are possible and should be included in H_b : Crystal-induced states due to the abrupt appearance of a periodic potential for $z \leq 0$ and polarization-induced (image) states due to quantum-mechanical exchange and correlation effects for $z > 0$. The former states are rather close to the surface whereas the latter extend deep into the plasma. Our exploratory calculation contains therefore only image states. To keep the mathematics as simple as possible we approximated moreover these states by classical image states, although this is not quite correct for the distances we are interested in. The wavefunctions for the approaching plasma electron are then Whittaker functions [3].

Plasma electrons loose/gain energy at metallic surfaces via creation/annihilation of internal electron-hole pairs. To describe this process we treat the metallic boundary as a jellium halfspace interacting with the electrons of the plasma via a screened Coulomb interaction: $V_s(r) \sim \exp[-(k_s)_{\text{surface}} r]/r$, where $(k_s)_{\text{surface}}$ is the screening wavenumber at the surface. To be consistent with the classical image states we have to assume an infinitely high barrier at $z = 0$. The wavefunctions for internal electrons are then standing waves and H_{e-b} can be worked out analytically [3].

If τ_e is sufficiently long, plasma electrons bound in image states are in thermal equilibrium with the surface. The desorption rate is then given by

$$\frac{1}{\tau_e} = \frac{\sum_{\vec{Q}n'} \sum_{\vec{Q}q} \exp[-\beta_s E_{\vec{Q}n'}] \mathcal{W}(\vec{Q}q, \vec{Q}'n')}{\sum_{\vec{Q}n} \exp[-\beta_s E_{\vec{Q}n}]}, \quad (4)$$

where $T_s = (k_B \beta_s)^{-1}$ is the surface temperature and $\mathcal{W}(\vec{Q}q, \vec{Q}'n')$ is the transition rate from the bound

surface state (\vec{Q}', n') , with \vec{Q}' the lateral momentum and n' the vertical quantum number, to the extended surface state (\vec{Q}, q) . The energy of the two states is, respectively, $E_{\vec{Q}'n'}$ and $E_{\vec{Q}q}$.

We calculated the transition rate $\mathcal{W}(\vec{Q}q, \vec{Q}'n')$ perturbatively as shown in Fig. 4. This is equivalent to an application of the golden rule and leads to (q and q' may label bound and extended surface states)

$$\mathcal{W}(\vec{Q}q, \vec{Q}'q') = \frac{2\pi}{\hbar} \sum_{\vec{K}\vec{K}'} \sum_{kk'} |\mathcal{V}_{\vec{Q}q, \vec{K}\vec{K}'}^{\vec{Q}'q'}|^2 \times n_F(E_{\vec{K}\vec{K}'}) [1 - n_F(E_{\vec{K}k})] \times \delta(E_{\vec{Q}'q'} + E_{\vec{K}\vec{K}'} - E_{\vec{Q}q} - E_{\vec{K}k}) \quad (5)$$

where $n_F(E)$ is the Fermi function for the metal electrons, with Fermi energy E_F and temperature T_s , $\mathcal{V}_{\vec{Q}q, \vec{K}\vec{K}'}^{\vec{Q}'q'}$ is the Coulomb matrix element describing the scattering of a plasma electron initially in state (\vec{Q}', q') on a metal electron initially in state (\vec{K}', k') , and $E_{\vec{K}\vec{K}'}$ is the energy of the electron in the metal.

For an electron in an extended surface state the tendency to stick to any bound surface state is

$$S_{\vec{Q}q} = \frac{16Lm_e a_B}{\hbar q'} \sum_{\vec{Q}n} \mathcal{W}(\vec{Q}n, \vec{Q}'q'), \quad (6)$$

where L is the width of the quantum-mechanical boundary layer (drops out for $L \rightarrow \infty$), m_e is the electron mass, and $\mathcal{W}(\vec{Q}n, \vec{Q}'q')$ is the transition rate from the extended surface state (\vec{Q}', q') to the bound surface state (\vec{Q}, n) . Provided extended surface states are Maxwellian occupied, with a temperature $T_e = (k_B \beta_e)^{-1}$, the angle and energy averaged sticking coefficient – the global sticking coefficient s_e – is

$$s_e = \frac{\sum_{\vec{Q}q'} S_{\vec{Q}q'} \exp[-\beta_e E_{\vec{Q}q'}]}{\sum_{\vec{Q}q} \exp[-\beta_e E_{\vec{Q}q}]}. \quad (7)$$

Subject to the constraints of the perturbative calculation of the transition rates, the functional form of Eqs. (4)–(7) is generic. With transition rates and single particle energies calculated from an appropriate microscopic model these formulas could be also applied to non-metallic boundaries.

3 Results [3]

Before we discuss results for s_e and τ_e a few remarks about $(k_s)_{\text{surface}}$ are in order. Little is known about this parameter except that it should be smaller than the bulk screening wavenumber $(k_s)_{\text{bulk}}$. Positron scattering experiments, for instance, indicate $(k_s)_{\text{surface}} \approx 0.6(k_s)_{\text{bulk}}$. For the results presented below we used this value for $(k_s)_{\text{surface}}$.

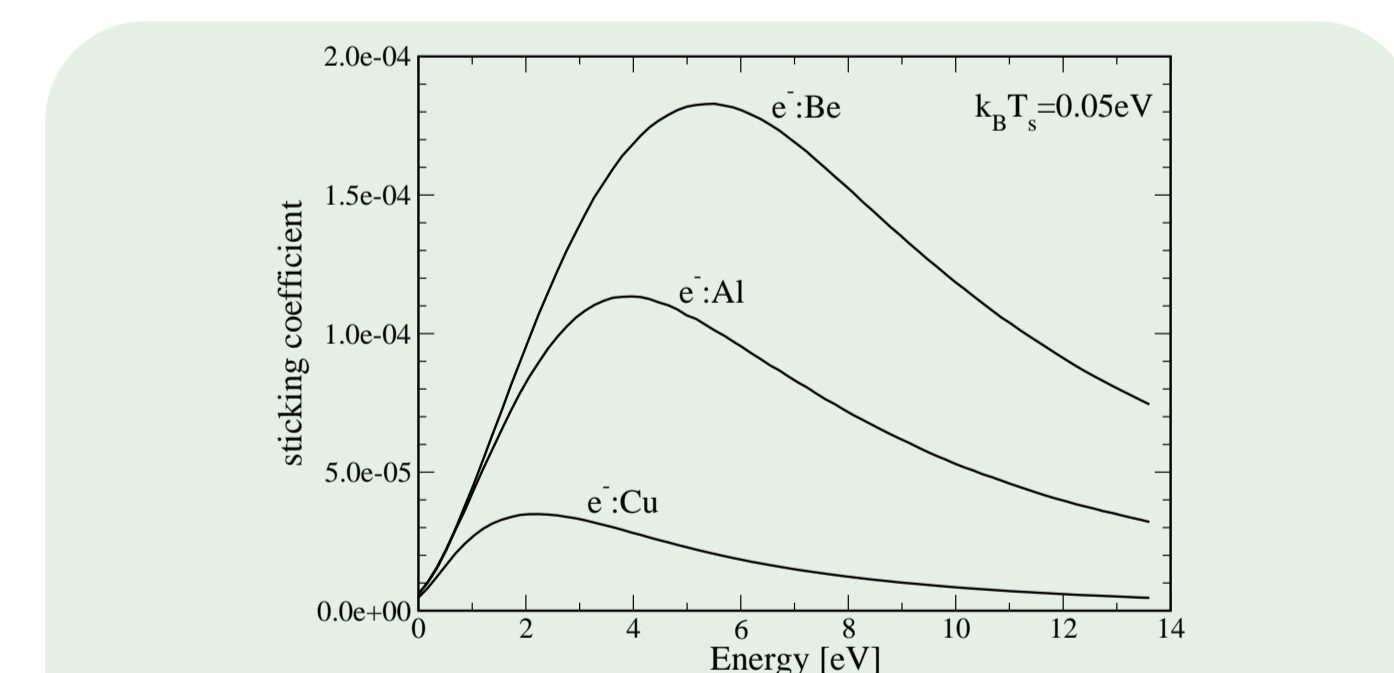


Fig. 5: Energy resolved sticking coefficient for plasma electrons hitting perpendicularly, respectively, a copper, an aluminum, and a beryllium surface at $k_B T_s = 0.05 \text{eV}$.

In addition we modified the binding energies of the surface states as obtained from the classical image potential by an overall factor of 0.7. This factor was chosen to adjust the binding energy of the lowest surface state $|E_1\rangle = 0.85 \text{eV}$ to the experimentally measured value for copper: $|E_1|^{\text{Cu}} \approx 0.6 \text{eV}$. Assuming this modification to approximately account for the deviation of the true polarization-induced potential from the classical image potential, we used this value also for the other metals.

Figure 5 shows the energy resolved sticking coefficient when the plasma electron perpendicularly hits, respectively, a copper, an aluminum, and a beryllium boundary at $k_B T_s = 0.05 \text{eV}$. With the proviso of the assumptions we made about the electronic structure of the plasma boundary and the modifications of the binding energies and the screening parameter, the sticking coefficient turns out to be extremely small, of the order of $10^{-5} - 10^{-4}$. For weaker screening, and thus stronger coupling, we would obtain sticking coefficients as large as 10^{-1} but these screening wavenumbers are unphysical. Global sticking coefficients defined in (7) are also very small (see Table 1). Although we cannot rule out that this is an artifact of our model, in particular, of our neglect of crystal-induced surface states, we also point out that the basis

of the widely accepted values $s_e \approx 0.1 - 1$ seems to be a semiclassical back-on-the-envelope approximation which does not withstand critical analysis [3].

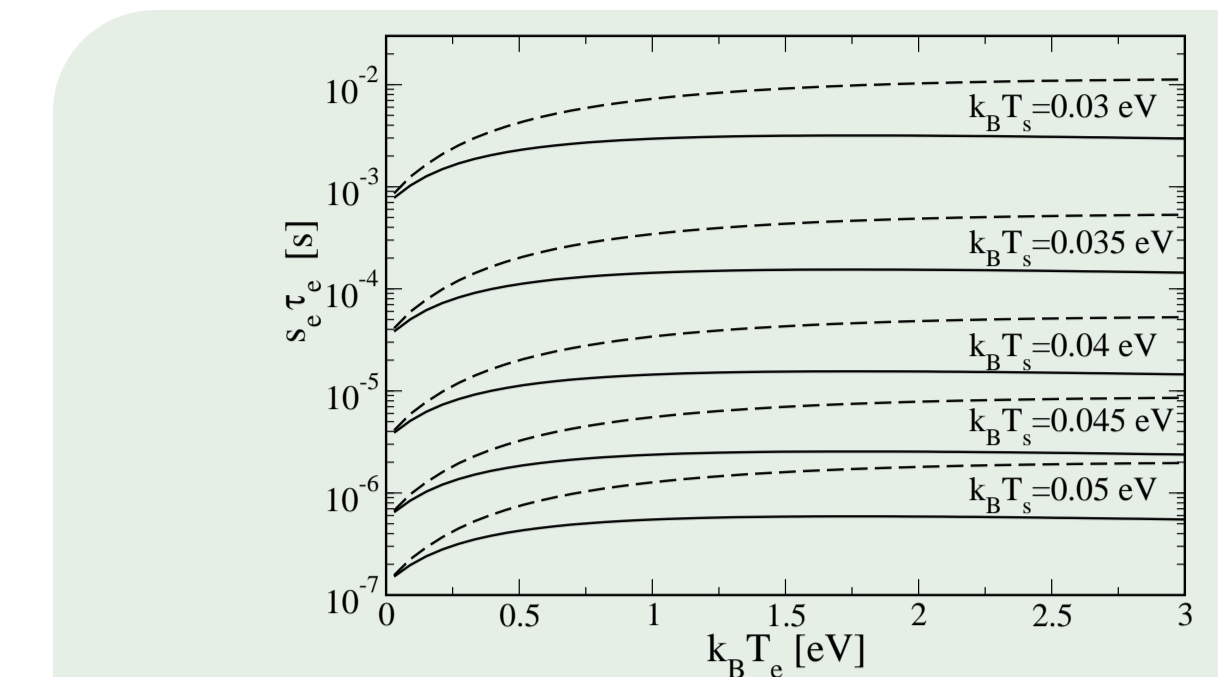


Fig. 6: The product $s_e \tau_e$ as a function of $k_B T_s$ for a thermal beam of plasma electrons hitting, respectively, a copper (full line) and a beryllium (dashed line) surface at various temperatures $k_B T_s$.

Desorption times τ_e obtained from Eq. (4) are of the order of 10^{-2} s (see Table 1). They are almost independent of $k_B T_e$, but strongly dependent on $k_B T_s$. For the surface model of the grain charge the product $s_e \tau_e$ is of central importance. We therefore plot in Fig. 6 directly this quantity, for thermal electrons hitting, respectively, a copper and a beryllium surface. Like τ_e , the product $s_e \tau_e$ depends only weakly on $k_B T_e$ but rather strongly on $k_B T_s$. Although s_e is in contradiction to what is generally assumed, $s_e \tau_e$ is of the expected order of magnitude. In particular, $s_e \tau_e$ for $k_B T_s \approx 0.05 \text{eV}$ would most probably produce charges for μm -sized metallic grains which are of the correct order of magnitude.

	Cu	Al	Be
τ_e [s]	0.026	0.021	0.022
s_e [10^{-5}]	1.8	5.6	8.9
$s_e \tau_e$ [10^{-6} s]	0.46	1.19	1.95

Table 1: Electron desorption time and global sticking coefficient for a thermal beam of plasma electrons with $k_B T_e = 5 \text{eV}$ hitting various metal surfaces at $k_B T_s = 0.05 \text{eV}$.

Let us finally mention that the phenomenological expression (2) cannot be rigorously obtained from Eqs. (4) and (7). Keeping however only a single bound state and assuming both the surface and the “relevant” electron temperature, which is not necessarily the electron temperature in the bulk of the discharge, to be much smaller than the binding energy of this state, we can show, applying Laplace’s approximation to the integrals (4) and (7), that

$$s_e \tau_e \approx \frac{16h}{(k_B T_s)^{3/2} (k_B \tilde{T}_e)^{-1/2}} \exp[\beta_s |E_1|], \quad (8)$$

which is identical to Eq. (2) when the relevant electron temperature \tilde{T}_e is of the order of T_s . The factor $16 = 8 \times 2$, which is absent in Eq. (2), is a consequence of the asymptotic form of the extended states of the classical image potential (factor 8) and of the fact that an electron approaching the grain boundary in an extended state can make a transition to any bound state on its way towards the surface and on its way back to the plasma (factor 2).

4 Summary

To support our surface model for the charge of a μm -sized grain in a gas discharge, which avoids treating the grain as a perfect absorber for electrons and ions and describes the build-up of surface charges as a physisorption process in the disturbed region of the grain, we investigated the microphysics of electrons at plasma boundaries.

Specifically, we calculated for a metallic boundary the electron sticking coefficient s_e and the electron desorption time τ_e assuming physisorption of electrons at metals to be controlled by electron-hole pair induced transitions between classical image states. Within this model, the sticking coefficient is unexpectedly small, $s_e \approx 10^{-4}$, indicating that the model is perhaps incomplete. On the other hand, the product $s_e \tau_e \approx 10^{-6}$ s for $k_B T_s \approx 0.05 \text{eV}$, which is the order of magnitude we would need to reproduce, for typical discharge conditions, the charge of a μm -sized metallic grain. Further studies are thus clearly needed to develop a consistent microscopic theory of particle charging.

5 References

- [1] F. X. Bronold et al., *Phys. Rev. Lett.* **101**, 175002 (2008).
- [2] F. X. Bronold et al., *Contrib. Plasma Phys.* **49**, 303 (2009).
- [3] F. X. Bronold et al., accepted by *Eur. Phys. J. D* (2009); arXiv:0901.4915.